CrystEngComm

COMMUNICATION

View Article Online
View Journal | View Issue

Cite this: *CrystEngComm*, 2017, **19**, 1156

Received 21st November 2016,
Accepted 6th January 2017

DOI: 10.1039/c6ce02418a

rsc.li/crystengcomm

Self-templating accelerates precipitation of carbamazepine dihydrate during the dissolution of a soluble carbamazepine cocrystal†

Hiroyuki Yamashita[ab] and Changquan Calvin Sun*[b]

Similarly organized carbamazepine (CBZ) clusters in a soluble cocrystal with glutaric acid templated the nucleation and precipitation of poorly soluble CBZ dihydrate during dissolution.

The use of highly soluble cocrystals is a promising strategy for enabling the delivery of poorly soluble drugs.[1–3] The key challenge in developing such soluble cocrystals is their tendency to undergo dissolution that is followed by the undesired precipitation of the poorly soluble parent drug, which negates the solubility advantage offered by the cocrystal. The precipitation of a less soluble solid phase of a drug is thermodynamically driven. When the concentration of a drug in solution, resulting from the dissolution of the soluble cocrystal, exceeds a certain concentration threshold, spontaneous crystallization of the poorly soluble parent drug commences. This leads to a decrease in solution concentration over time and yields a solution concentration–time profile described as the spring and parachute effect.[4] When precipitation occurs quickly, the precipitate may cover the surfaces of the soluble crystals formed so that the observed dissolution rate is equivalent to that of the parent drug, which is low. Elimination or even delaying such an undesired phase change of the cocrystal during dissolution depends on the successful control of crystallization kinetics, especially nucleation of the less soluble phase.

A commonly used strategy to inhibit nucleation and growth in solution crystallization is the use of tailor-made additives. Specific interactions between the additive and the crystallized molecules can be employed to inhibit the crystallization of one polymorph and allow the preparation of another polymorph that is otherwise difficult to obtain as a pure phase.[5–7] Successful surface templating using polymers,[8] crystals,[9] and 2D surfaces[10] has been demonstrated. For example, some crystals act as heterogeneous nucleation substrates for the epitaxial growth of other crystals.[11] Seeding with hetero molecules was used to obtain some elusive crystals.[12–14] A computational approach was also employed to facilitate the design of hetero nucleation.[15–17]

Here we report a new mode of nucleation templating where the soluble multi-component crystal itself acts as a nucleation template to induce facile precipitation of the poorly soluble individual components, a phenomenon termed self-nucleation hereafter. Considering two soluble cocrystals of the same drug, the one with a higher solubility corresponds to a higher thermodynamic driving force and, hence, a greater tendency to crystallization of the poorly soluble parent drug from the solution saturated by the more soluble cocrystal. We have discovered a counterintuitive example, where a more soluble cocrystal of carbamazepine (CBZ) is kinetically more stable than a less soluble cocrystal. Further investigation reveals a self-templating mechanism that accelerated the nucleation of the less soluble CBZ dihydrate crystal.

Dissolution behavior of CBZ 1:1 cocrystals with nicotinamide (CBZ-NCT)[18] and glutaric acid (CBZ-GLA)[19] was studied. The aqueous solubility of CBZ-NCT and CBZ-GLA is 70 mM and 54 mM, respectively.[2] Therefore, with respect to CBZ dihydrate (solubility is 0.46 mM), the degree of supersaturation in the diffusion layer of CBZ-NCT is ~30% higher than that of CBZ-GLA because the concentration of solute molecules in the diffusion layer is saturated with respect to the dissolving crystal.[20] When the CBZ-GLA cocrystal was dissolved into a pH 6.8 phosphate buffer (the medium used in the dissolution experiments) to form a 54 mM solution, the solution pH decreased to 3.9. This pH shift, which may be expected in the diffusion layer, changed the solubility of CBZ-GLA to 63 mM,[21] which is still lower than that of CBZ-NCT. Therefore, faster conversion to the dihydrate may be expected for CBZ-NCT based on the more favorable

[a] *Analytical Research Laboratories, Technology, Astellas Pharma Inc., Tsukuba-shi, Ibaraki, 305-8585, Japan*
[b] *Pharmaceutical Materials Science and Engineering Laboratory, Department of Pharmaceutics, College of Pharmacy, University of Minnesota, Minneapolis, MN 55455, USA. E-mail: sunx0053@umn.edu*

† Electronic supplementary information (ESI) available: Materials and methods, including the parameters used in crystal lattice matching and structure similarity analysis. See DOI: 10.1039/c6ce02418a

thermodynamic driving force. During dissolution of both neat cocrystals in water, a layer of CBZ dihydrate precipitates out and covers the surface of the cocrystal pellet so that the measured intrinsic dissolution rates (IDR) of the two cocrystals are the same as that of the CBZ dihydrate (Fig. 1a and b). Thus, different nucleation kinetics could not be easily observed.

Thermodynamically driven phase transformations can be manipulated kinetically. For example, crystallization inhibitors can be used to prolong the nucleation induction time,[22] and chemical impurities can be used to slow down the nucleation of the more stable form.[23] Hydroxypropyl methylcellulose acetate succinate (HPMCAS), a polymer that effectively inhibits the crystallization kinetics of many drugs,[24] was used to retard the crystallization in the two CBZ cocrystal systems with 3 : 1, 1 : 1 and 1 : 3 (w/w) ratios. Mixtures were prepared by gently milling with a mortar and pestle, followed by compaction to form pellets for IDR experiments. In the phosphate buffer (pH 6.8), the IDR of CBZ-NCT was much greater with HPMCAS, indicating its effectiveness in inhibiting the nucleation of CBZ dihydrate (Fig. 1a). The 1 : 1 cocrystal to HPMCAS ratio yielded a higher IDR than the 1 : 3 ratio for two possible reasons: a) the higher polymer amount effectively reduced the area of CBZ-NCT exposed to the dissolution medium by the effect of dilution, and b) the higher amount of polymer might have led to higher viscosity in the diffusion layer, which reduced the diffusion of the CBZ molecules into the bulk medium. However, the higher variability in dissolution data of the 1 : 1 mixture indicates inadequate inhibition of nucleation of CBZ dihydrate during dissolution. In fact, the 3 : 1 and 1 : 1 physical mixtures of CBZ-NCT and HPMCAS transformed into CBZ dihydrate in a few minutes, but the 1 : 3 mixture exhibited no detectable phase transformation (Fig. 2a). Pellets of the 1 : 3 mixture did not appear highly crystalline because the dominating polymer phase is amorphous instead of amorphization of the cocrystal by grinding.

Surprisingly, no improvement in the IDR of CBZ-GLA with HPMCAS was observed even for the 1 : 3 mixture, despite its lower degree of supersaturation than CBZ-NCT (Fig. 1b). The CBZ-GLA transformed immediately to CBZ dihydrate even in the

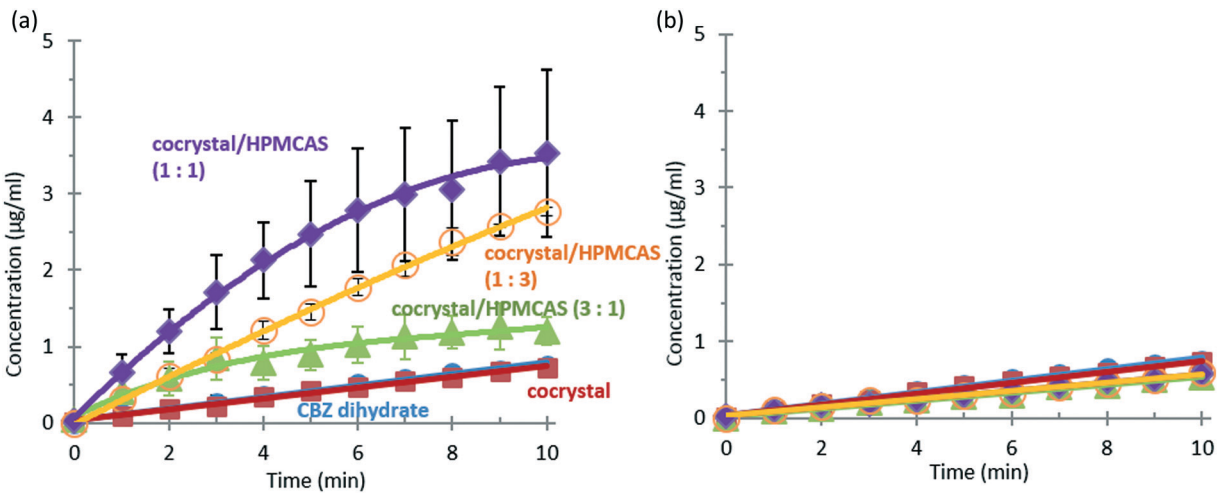

Fig. 1 Stability difference from results of IDR between (a) CBZ-NCT and (b) CBZ-GLA cocrystals (n = 3).

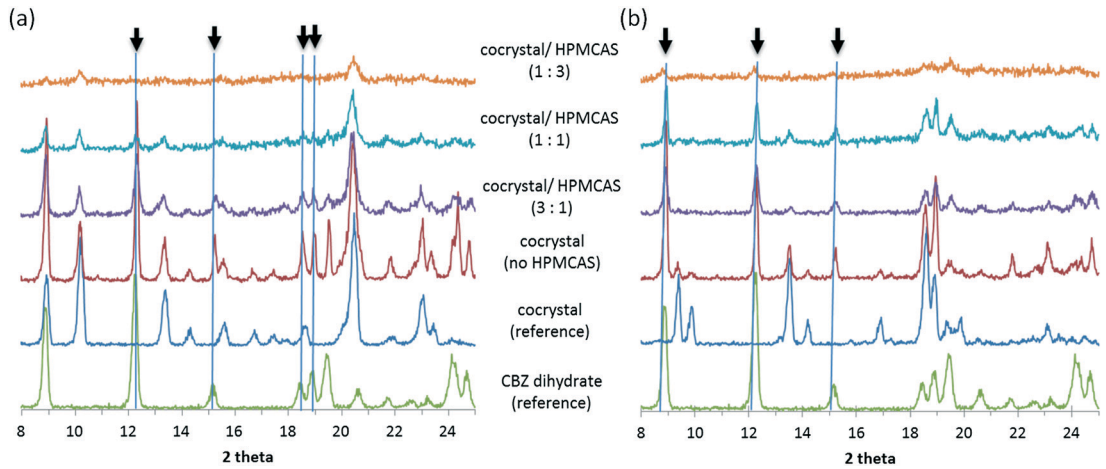

Fig. 2 X-ray diffraction patterns of pellets after IDR for 10 min. Black arrows indicate typical peaks of CBZ dihydrate. (a) CBZ-NCT and (b) CBZ-GLA with various amounts of HPMCAS.

presence of a high level of HPMCAS, which is effective in inhibiting the nucleation of CBZ dihydrate from solution in the case of CBZ-NCT. Powder X-ray diffraction patterns of the pellets after IDR experiments showed mixed patterns of the cocrystal and CBZ dihydrate (Fig. 2). These results suggest that CBZ-GLA is kinetically less stable than CBZ-NCT despite the lower degree of supersaturation in the diffusion layer.

Pair-wise analysis of crystal packing similarity was performed using Mercury (v.3.8 CCDC, UK). The 3D spatial arrangement of CBZ molecules in the CBZ dihydrate structure is very similar to that in CBZ-GLA but quite different from that in CBZ-NCT (Fig. 3). The structure similarity analysis results (Table 1) show that 7 and 6 out of the 20 CBZ molecules met the tolerance criteria for CBZ-GLA and CBZ-NCT, respectively. Among the molecules that do meet the criteria, the root mean square (RMS) distance between CBZ-NCT and CBZ dihydrate is more than 2 fold that between CBZ-GLA and CBZ dihydrate. Thus, CBZ-GLA is structurally much more similar to CBZ dihydrate than CBZ-NCT.

In the dihydrate crystal structure, water molecules and the amide functional groups of CBZ are hydrogen bonded to form 2D layers, where the hydrophobic backbone of CBZ molecules are pegged on either side of this layer to form a hydrophobic surface. The 2D layers stack to yield the 3D packing of the dihydrate (Fig. 4a). There is no hydrogen bonding between adjacent CBZ molecules (Fig. 5a). In the CBZ-GLA crystal structure, GLA molecules are connected through hydrogen bonds to form a 2D layer, where the CBZ molecules are also pegged along the sides of the 2D layer with CBZ pairs in a nearly identical arrangement to those in the dihydrate (Fig. 4b) without hydrogen bonding (Fig. 5b). In the CBZ-NCT crystal structure, CBZ molecules form dimers through intermolecular hydrogen bonds (Fig. 5c), which further connect to form a 1D column. In this structure (Fig. 4c), CBZ molecules form dimers with a distinct structure from that observed in the dihydrate and CBZ-GLA (Fig. 5).

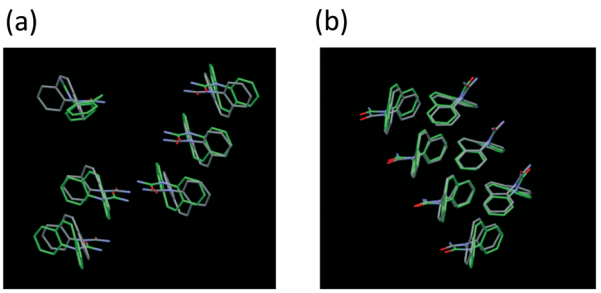

Fig. 3 Comparison of crystal structures between CBZ dihydrate (grey) and a cocrystal (green) of (a) CBZ-NCT or (b) CBZ-GLA.

Table 1 Summary of the difference between CBZ-NCT and CBZ-GLA cocrystals

	CBZ-NCT	CBZ-GLA
Solubility (mM) (ref. 2)	70	54
IDR of 1 : 3 (w/w) cocrystal and HPMCAS mixture (μg cm^{-2} min^{-1})	298.0	46.7
Root mean square in distance (Å) (molecules in common)	1.45 (6)	0.60 (7)

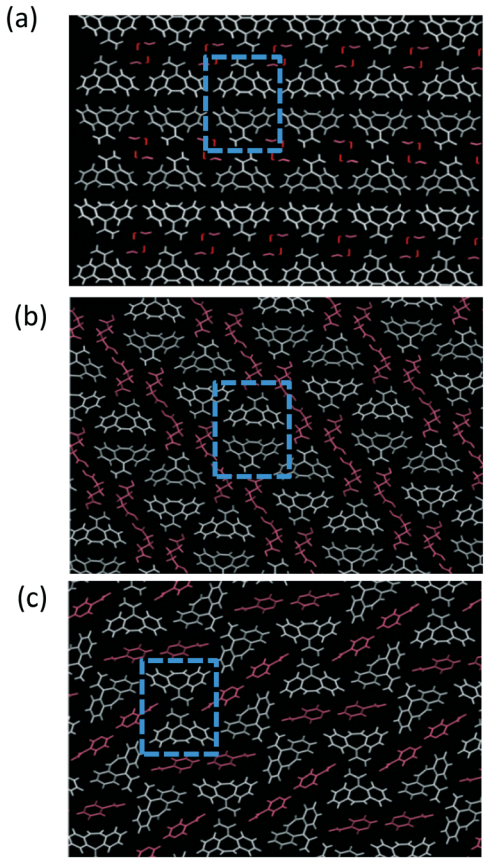

Fig. 4 Comparison of the crystal structures of a) CBZ dihydrate, b) CBZ-GLA, and c) CBZ-NCT. One CBZ dimer in each crystal structure is highlighted in the box.

This result is consistent with an earlier analysis of the structure similarity among known crystal forms of CBZ using a sophisticated analysis algorithm, where it was shown that CBZ dihydrate was structurally more similar to CBZ-GLA than CBZ-NCT.[26] We speculate that, during the dissolution of CBZ-GLA, the more hydrophilic GLA molecules tend to leave the crystal surface more readily because of its stronger

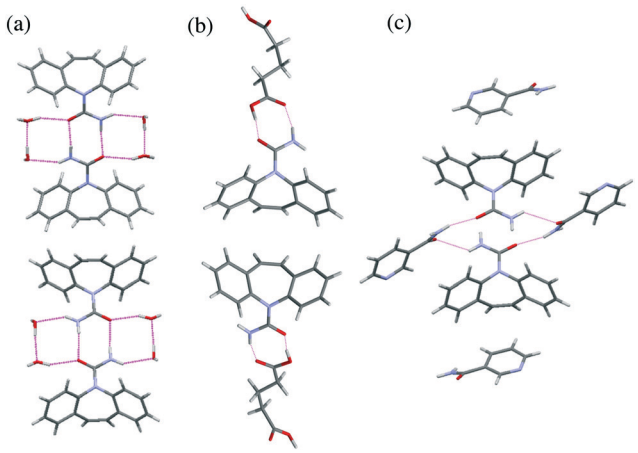

Fig. 5 Comparison of CBZ pairs of a) CBZ dihydrate, b) CBZ-GLA, and c) CBZ-NCT.

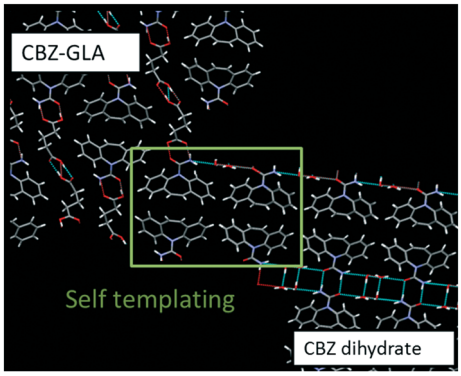

Fig. 6 Image of self-templating between CBZ-GLA and CBZ dihydrate.

interaction with water and its higher aqueous solubility than CBZ. This leaves the surface of the CBZ-GLA crystal enriched with such CBZ pairs. Such a surface likely serves as an excellent template for the growth of CBZ dihydrate. Therefore, crystallization of CBZ dihydrate can occur more easily even under a lower degree of supersaturation than CBZ-NCT. This is analogous, but mechanistically distinct, to the enantioselective nucleation of leucine on a self-assembled monolayer.[25] Crystal lattice matching analysis using the GRACE software did not suggest better lattice matching of the CBZ dihydrate with CBZ-GLA than CBZ-NCT (Fig. S1†). Thus, the more effective nucleation by CBZ-GLA cannot be attributed to epitaxial growth of the CBZ dihydrate. Rather, the similar CBZ molecular packing is responsible for it. CBZ cocrystals with maleic acid, oxalic acid, and tartaric acid were categorized into the same structure group as CBZ dihydrate.[26] Thus, they may also exhibit the self-templating phenomenon observed for CBZ-GLA. Fig. 6 shows the most energetically favored growth direction of CBZ dihydrate because of the presence of two hydrogen bonded chains. The templating of CBZ dihydrate by CBZ-GLA explains the apparent ineffectiveness of HPMCAS, a nucleation inhibitor, in stabilizing CBZ-GLA during dissolution. This is a case where crystallization kinetics dominates over thermodynamics.

In conclusion, the evidence suggests that the mechanism of self-templated nucleation, due to the similar arrangement of CBZ on the surface of CBZ-GLA and CBZ dihydrate, explains the unexpected fast precipitation of CBZ dihydrate during the dissolution of CBZ-GLA despite its lower thermodynamic driving force and the presence of a nucleation inhibitor. This mechanism has implications in the development and stabilization of more soluble crystal forms of drugs for improved drug delivery performance. For cases that involve self-templated nucleation, stabilization should be focused on inhibiting crystal growth of the precipitating crystals since nucleation inhibition is unlikely to be effective.

References

1 D. P. McNamara, S. L. Childs, J. Giordano, A. Iarriccio, J. Cassidy, M. S. Shet, R. Mannion, E. O'Donnell and A. Park, *Pharm. Res.*, 2006, **23**, 1888–1897.
2 D. J. Good and N. Rodriguez-Hornedo, *Cryst. Growth Des.*, 2009, **9**, 2252–2264.
3 G. Bolla, P. Sanphui and A. Nangia, *Cryst. Growth Des.*, 2013, **13**, 1988–2003.
4 J. Brouwers, M. E. Brewster and P. Augustijns, *J. Pharm. Sci.*, 2009, **98**, 2549–2572.
5 I. Weissbuch, L. Leisorowitz and M. Lahav, *Adv. Mater.*, 1994, **6**, 952–956.
6 R. J. Davey, N. Blagden, G. D. Potts and R. Docherty, *J. Am. Chem. Soc.*, 1997, **119**, 1767–1772.
7 Y. Gong, B. M. Collman, S. M. Mehrens, E. Lu, J. M. Miller, A. Blackburn and D. J. W. Grant, *J. Pharm. Sci.*, 2008, **97**, 2130–2144.
8 C. P. Price, A. L. Grzesiak and A. J. Matzger, *J. Am. Chem. Soc.*, 2005, **127**, 5512–5517.
9 C. A. Mitchell, L. Yu and M. D. Ward, *J. Am. Chem. Soc.*, 2001, **123**, 10830–10839.
10 C. Capacci-Daniel, K. J. Gaskell and J. A. Swift, *Cryst. Growth Des.*, 2010, **10**, 952–962.
11 N. Rodriguezhornedo, D. Lechugaballesteros and H. J. Wu, *Int. J. Pharm.*, 1992, **85**, 149–162.
12 F. P. A. Fabbiani, G. Buth, D. C. Levendis and A. J. Cruz-Cabez, *Chem. Commun.*, 2014, **50**, 1817–1819.
13 D. K. Bucar, G. M. Day, I. Halasz, G. G. Z. Zhang, J. R. G. Sander, D. G. Reid, L. R. MacGillivray, M. J. Duer and W. Jones, *Chem. Sci.*, 2013, **4**, 4417–4425.
14 T. Friscic and L. R. MacGillivray, *Chem. Commun.*, 2009, 773–775, DOI: 10.1039/b820120j.
15 S. L. Price, D. E. Braun and S. M. Reutzel-Edens, *Chem. Commun.*, 2016, **52**, 7065–7077.
16 J. B. Arlin, L. S. Price, S. L. Price and A. J. Florence, *Chem. Commun.*, 2011, **47**, 7074–7076.
17 V. K. Srirambhatla, R. Guo, S. L. Price and A. J. Florence, *Chem. Commun.*, 2016, **52**, 7384–7386.
18 N. Rodriguez-Hornedo, S. J. Nehru, K. F. Seefeldt, Y. Pagan-Torres and C. J. Falkiewicz, *Mol. Pharmaceutics*, 2006, **3**, 362–367.
19 S. L. Childs, N. Rodriguez-Hornedo, L. S. Reddy, A. Jayasankar, C. Maheshwari, L. McCausland, R. Shipplett and B. C. Stahly, *CrystEngComm*, 2008, **10**, 856–864.
20 W. Nernst, *Z. Phys. Chem., Stoechiom. Verwandtschaftsl.*, 1904, **47**, 52–55.
21 S. J. Bethune, N. Huang, A. Jayasankar and N. Rodriguez-Hornedo, *Cryst. Growth Des.*, 2009, **9**, 3976–3988.
22 G. A. Ilevbare, H. Y. Liu, K. J. Edgar and L. S. Taylor, *Cryst. Growth Des.*, 2013, **13**, 740–751.
23 C. H. Gu, K. Chatterjee, V. Young and D. J. W. Grant, *J. Cryst. Growth*, 2002, **235**, 471–481.
24 H. Konno, T. Handa, D. E. Alonzo and L. S. Taylor, *Eur. J. Pharm. Biopharm.*, 2008, **70**, 493–499.
25 N. Banno, T. Nakanishi, M. Matsunaga, T. Asahi and T. Osaka, *J. Am. Chem. Soc.*, 2004, **126**, 428–429.
26 S. L. Childs, P. A. Wood, N. Rodriguez-Hornedo, L. S. Reddy and K. I. Hardcastle, *Cryst. Growth Des.*, 2009, **9**, 1869–1888.